Torsion, twist, and writhe: the elementary geometry of axonemal bending in three dimensions

Division of Biology, California Institute of Technology

Part 1. Statics

The cilia and flagella of eukaryotic cells function by active bending that produces cell movements and fluid flows in their environment. They contain a common cytoskeleton, known as the axoneme, that is the locus of all the enzymes and mechanical components that are required for production of useful bending. The bending of many flagella, and some cilia, is planar, or at least nearly planar. In these cases, the usual observation is that bends are formed near the basal end and then propagate towards the tip. The flagellum of a sea urchin spermatozoon is a classic example [Gray, 1955; Brokaw, 1990]. Planar bending is easy to record as planar photographic images, and is mathematically simple. The shape of the bent flagellum can be described mathematically by a scalar variable, ϕ, that measures the curvature of the flagellum as a function of length along the flagellum.

There are also many cilia and flagella that generate bending in 3 dimensions. These bending patterns are more difficult to record and analyze, and their mathematical description is more complex. However, it is important to understand this complexity in order to understand how a flagellum generates 3-dimensional bending. The pioneering analysis is the paper by Hines and Blum [1983], and to the extent possible, their conventions have been followed here.

Mathematical analysis of 3-dimensional bending is simplified by restricting attention to bending of a structure such as a flagellum. Neglecting pathological cases where a flagellum is broken, the elastic bending resistance of the flagellum smooths its bends so that its curvature is a continuous function of length. Restricting the analysis of 3-dimensional bending to cases where the curvature is always greater than 0 (except possibly at the ends of the flagellum), is sufficient to handle most cases of flagellar bending.

1.1 Curvature and torsion of a space curve

1.1.1 The Frenet-Serret apparatus

A curve in space can be defined by a continuous series of points $\mathbf{P}(s)$ where $\mathbf{P}$ represents a vector from the origin of a global XYZ coordinate system. The parameter s measures arc length along the curve. At any point, the tangent to the curve is a vector $\mathbf{t} = d\mathbf{P}/ds$, and since s is arc length,

t is a unit vector.

The curvature of a space curve is a scalar function $\kappa(s)$ defined by

$$d\mathbf{t}/ds = d^2\mathbf{P}/ds^2 = \kappa \mathbf{n}, \quad (1)$$

where **n** is a unit vector perpendicular to the tangent **t** , pointing towards the center of the circle of curvature. This direction is obtained by straightforward vector subtraction:

$$\kappa \mathbf{n} = \lim_{(\Delta s \to 0)} (\mathbf{t}\,[s+\Delta s] - \mathbf{t}\,[s])/\Delta s. \quad (2)$$

The binormal vector, **b**, is defined as

$$\mathbf{b} = \mathbf{t} \times \mathbf{n}. \quad (3)$$

The vectors **t n b**, specified in that order, are an orthogonal triad of unit vectors, known as the Frenet triad, which defines a local coordinate system at every point along the length of the curve. Since **t** and **n** are both unit vectors, and are perpendicular to each other, equation (3) establishes that **b** is a unit vector, perpendicular to the plane of **t** and **n**, so the triad is orthogonal. (See insert 1 and Figure 1)

The change in this local coordinate system as it moves along the curve can be described by the Frenet-Serret equations:

$$\begin{aligned} d\mathbf{t}/ds &= \kappa \mathbf{n}, \\ d\mathbf{n}/ds &= -\kappa \mathbf{t} + \tau \mathbf{b}, \\ d\mathbf{b}/ds &= -\tau \mathbf{n}. \end{aligned} \quad (4)$$

The new scalar variable, τ, is the torsion of the curve. Equation (4) tells us that the two scalar functions $\kappa(s)$ and $\tau(s)$ are sufficient to describe the change in the local coordinate system as it moves along the curve, and therefore are sufficient to describe the shape of the curve.

1.1.2 Generalized rotation

A more general approach starts by defining a local x y z coordinate system at each point along the length of a space curve. U(s) at each point is a set of unit vectors $\{\mathbf{u}_x, \mathbf{u}_y, \mathbf{u}_z\}$ for each of the coordinate axes. We choose to orient the coordinate system with its z axis along the space curve, that is $\mathbf{u}_z = \mathbf{t}$. In general, U(s) will rotate as it moves from point to point along the curve. At any

point, its rate of rotation can be described by an angular velocity vector ω which has a direction along the axis of rotation, perpendicular to the plane in which rotation is occuring. We can write

$$dU/ds = \omega \mathbf{X} U, \tag{5}$$

as shorthand notation for

$$\begin{aligned} d\,\mathbf{u}_x/ds &= \omega \mathbf{X} \mathbf{u}_x = +\omega_z \mathbf{u}_y - \omega_y \mathbf{u}_z \\ d\,\mathbf{u}_y/ds &= \omega \mathbf{X} \mathbf{u}_y = -\omega_z \mathbf{u}_x + \omega_x \mathbf{u}_z \\ d\,\mathbf{u}_z/ds &= \omega \mathbf{X} \mathbf{u}_z = +\omega_y \mathbf{u}_x - \omega_x \mathbf{u}_y. \end{aligned} \tag{6}$$

To obtain the first of these equations, note that rotation around the x axis (ω_x) does not change the position of the end of $\mathbf{u}_x$. Using the right-hand rule, rotation around the z axis (ω_z) moves the end of the $\mathbf{u}_x$ in the +y direction, at a velocity = $\omega_z u_x = \omega_z$, so this gives a term $\omega_z \mathbf{u}_y$. Similarly, rotation around the y axis (ω_y) moves the end of $\mathbf{u}_x$ in the -z direction, giving a term $-\omega_y \mathbf{u}_z$. The other two equations can be obtained in the same manner.

Insert 1: Vector multiplication

The operator ● represents the scalar product, or dot product, of two vectors **a** and **b**. The result is a scalar quantity c that is proportional to the cosine of the angle between **a** and **b**.

$$\mathbf{c} = \mathbf{a} \bullet \mathbf{b} = a_x b_x + a_y b_y + a_z b_z = |\mathbf{a}||\mathbf{b}| \cos \theta_{ab}. \tag{7}$$

Note that the magnitude of a vector = $|\mathbf{a}| = \mathrm{sqrt}(\mathbf{a} \bullet \mathbf{a})$, and if c=0, the two vectors **a** and **b** are perpendicular.

The operator **X** represents the vector product, or cross product, of two vectors **a** and **b**. The result is a new vector **c** that is perpendicular to the plane containing **a** and **b**, with a direction such that the triad **a b c** is right-handed triad. The magnitude of **c** is proportional to the sine of the angle between **a** and **b**. The general formula for calculating the components of $\mathbf{c} = \mathbf{a} \mathbf{X} \mathbf{b}$ is:

$$\begin{aligned} c_x &= a_y b_z - a_z b_y, \\ c_y &= a_z b_x - a_x b_z, \\ c_z &= a_x b_y - a_y b_x. \end{aligned} \tag{8}$$

These equations can be used to obtain equation (6), and also to show that the unit vectors of the **x y z** coordinate system are related by $\mathbf{u}_z = \mathbf{u}_x \times \mathbf{u}_y$, $\mathbf{u}_x = \mathbf{u}_y \times \mathbf{u}_z$, and $\mathbf{u}_y = -\mathbf{u}_x \times \mathbf{u}_z$. The foregoing is based on the assumption that the **x y z** coordinate system was defined as a right-handed triad.

Since $\mathbf{t} = \mathbf{u}_z$, it is easy to see that if $\omega_x = 0$, the Frenet-Serret equations (4) are a special case of equations (6), with $\dot{\mathbf{n}} = \omega_y \mathbf{u}_x$, $\mathbf{b} = \mathbf{u}_y$, and $\dot{\mathbf{n}} = -\omega_z \mathbf{u}_x$. Since $\kappa = \omega_y$, we can consider the curvature to be a vector $\boldsymbol{\kappa} = \omega_y \mathbf{u}_y = \kappa \mathbf{b}$, and similarly the torsion can be considered to be a vector $\boldsymbol{\tau} = \omega_z \mathbf{u}_z = \tau \mathbf{t}$. With $\omega_x = 0$, the total angular velocity is

$$\boldsymbol{\omega} = \omega_y \mathbf{u}_y + \omega_z \mathbf{u}_z = \boldsymbol{\kappa} + \boldsymbol{\tau} = \kappa \mathbf{b} + \tau \mathbf{t} = \mathbf{D}. \qquad (9)$$

When written in the form $\kappa \mathbf{b} + \tau \mathbf{t}$, the total angular velocity is referred to as the Darbaux vector, represented here as **D** [Goetz, 1970].

In the more general case, when ω_x is not 0, the curvature vector, $\boldsymbol{\kappa}$, which must be perpendicular to **t**, is in the x,y plane and $\boldsymbol{\kappa} = \boldsymbol{\kappa}_x + \boldsymbol{\kappa}_y = \kappa_x \mathbf{u}_x + \kappa_y \mathbf{u}_y = \kappa_x \mathbf{u}_x + \omega_y \mathbf{u}_y$. Let θ be the angle between $\boldsymbol{\kappa}$ and $\mathbf{u}_x$. The case where θ is constant along s is of little interest; it is simpler to redefine the x y z system so that $\omega_x = 0$. It is more useful to interpret the x y z coordinate system as a system that is fixed in the material of a structure that is bending to form the space curve, and refer to it as the body coordinate system. In this case, the torsion is interpreted as rotation of the curvature vector in the x,y plane of the body coordinate system:

$$d\theta/ds = \tau. \qquad (10)$$

Specification of $\boldsymbol{\kappa}(s)$ as a vector function of arc length determines $\kappa(s)$, and therefore $\tau(s)$, and is sufficient to define the curve.

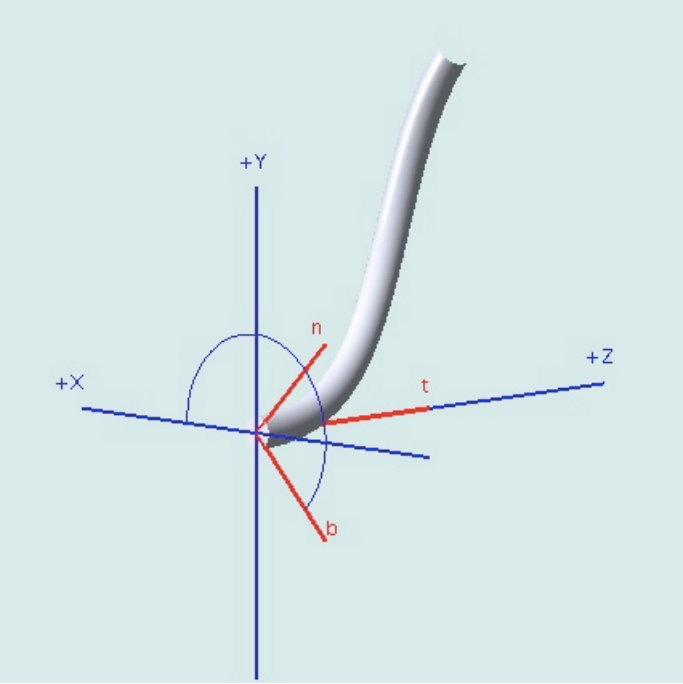

Figure 1. Three-dimensional view of the coordinate systems for a space curve, which is the axis of the bent cylinder shown in this figure. The x, y plane is perpendicular to the curve, as is the **n**, **b** plane. The tangent to the curve is in the **t** and +z directions. The curvature vector is in the **b** direction, and the angle ϕ is represented by the blue arc drawn from the +x axis to the **b** vector.

1.2 The Circular Helix

A particularly simple curve defined by κ and τ is the circular helix, which results when the values of κ and τ are constant and non-zero. The axis of the helix is parallel to the Darbaux vector. The standard parameters of the helix, the radius, r, and the pitch, h, are given by

$$r = \kappa /(\kappa^2 + \tau^2) \quad \text{and} \quad h = 2\pi\tau/(\kappa^2 + \tau^2) . \tag{11}$$

The pitch angle ϕ_H is the angle between the tangent and the Darbaux vector, and is given by

$$\tan(\phi_H) = 2\pi r/h = \kappa / \tau \tag{12}$$

The arc length in one turn of the helix is S:

$$S = \text{sqrt} ((2\pi r)^2 + h^2). \tag{13}$$

The position components of points on the curve, in a global X Y Z coordinate system, are given by

$$X = -r \sin(2\pi s/S), \quad Y = r \cos(2\pi s/S), \quad Z = hs/S. \tag{14}$$

This representation produces a right-handed helix starting at {0, r, 0} and aligns the Darbaux vector and the axis of the helix with the Z coordinate axis.

When the curvature is specified as a vector function of s, a circular helix results when the components of the curvature vector are {□cos(□s), □□sin(□s), 0}.

These equations give a right-handed helix, when □, □, r, and h are all positive. Negative values of torsion produce a left-handed helix, and suggest that the pitch should also be negative. If the pitch is negative, S should also be negative, and the effect is then just to change the sign of the X term in equation (14).

1.3 Twist

In order to discuss twist, it is necessary to go beyond the idea of a space curve and describe a structure that is following a space curve. The simplest structure, a ribbon, is often used by mathematicians to illustrate such discussions, but here we will use a cylinder, with one or more elements specified on the surface of the cylinder. This structure resembles the internal cytoskeleton of cilia and flagella, known as the axoneme, which usually is a cylinder with 9 outer microtubular doublets. Of course, the axis of the cylinder and any one of the elements define a ribbon, of constant width. The axis of the cylinder is a space curve, and when we refer to the curvature or torsion of the cylinder we are referring to the curvature or torsion of this space curve. Now consider that we have a straight cylinder, and apply equal and opposite torques, or moments, to each end, so that one end of the cylinder rotates relative to the other end, while the cylinder remains straight (no bending). If this rotation were to occur while the two end surfaces of the cylinder remain planar and parallel, the elements on the surface must become longer than the axis of the cylinder. If the elements on the surface retain constant length, the ends of the cylinder must be deformed. So twisting requires strain within the cylinder, and will be resisted by the elastic resistances of the material of the cylinder. This resistance will be referred to as the elastic twist resistance, without determining whether it results from stretch resistance or shear resistance of the material, or a combination of both. If the moments are removed, the torque produced by the elastic twist resistance will reverse the original rotation and the cylinder will return to its original configuration.

What is the relation between twist and torsion? To examine this, the body coordinate system of the cylinder, described in Section 1.1.2, is used. The z axis of the body system lies along the axis of the cylinder, and a particular element is chosen that is always on the +y axis. So, if the cylinder is

twisted, the body coordinate system rotates locally around the z axis. To finish the definition of this coordinate system, a "basal" end of the cylinder is defined, at which arc length s along the cylinder = 0. Then z and s increase in the same direction, from base to "tip" of the cylinder. The direction of the x coordinate is then specified for a right-handed x y z coordinate system, as shown in Figure 1. Since the Frenet-Serret system is a right-handed system with z increasing in the +s direction, **n** and **b** must always lie in the x,y plane, and when **n** is in the y direction, **b** must be in the –x direction. In an untwisted cylinder, rotation of the curvature vector by the torsion must cause rotation of the curvature vector in the x,y plane. The position of the curvature vector is specified by an angle ϕ measured from the x axis towards the y axis (Figure 1), and the torsion is then $d\phi/ds$, as in equation (10). However, if the cylinder is twisted, as described in the preceding paragraph, this twist will cause an additional rotation of the curvature vector, resulting from rotation of the x y z coordinate system. In general then

$$\text{torsion } \tau = d\phi/ds + \tau_z, \tag{15}$$

where the curvature τ_z measures the rate of change of twist angle along the length [Gueron and Liron, 1993]. Twist is torsion, but not all torsion is twist. In many contexts, the terms twist and torsion are used interchangably. In the absence of bending, this causes no problems. However, with flagella and cilia, where bending is important, it is preferable to use the term twist to refer to twist, and not complicate the interpretation by referring to twist as torsion.

Twist of an axoneme could be generated by mechanisms other than application of external torque. The internal motors, known as dyneins, that generate flagellar bending generate sliding forces between the outer doublets. If these forces are parallel to the doublets, they generate negligible twisting moments [Hines and Blum, 1984]. However, observations of in vitro movement of microtubules by dyneins show microtubule rotation, indicating that dyneins can, under some circumstances, produce twisting moments. Twist resulting from such internal twisting moments will be resisted by the elastic twist resistance of the axoneme. If generation of moments by the dyneins is terminated, the elastic twist resistance of the axoneme will restore its untwisted conformation. Alternatively, twist of the axonemal components might be a built-in, permanent, feature of the structure, which is independent of moments generated by the dyneins or applied externally. Most cilia and flagella do not show evidence of built-in twist, and the doublets of an inactive flagellum appear to run straight along the axoneme, as elements of a cylinder. However, exceptions are found in the flagella of a few types of insect sperm [Phillips, 1969, 1971].

1.4 Transformation and rotation

Given two coordinate systems U_1 and U_2, and a vector $\mathbf{v}$ specified by its coordinates in one of these systems, eg. $\mathbf{v}_1 = \{v_{1x}\mathbf{u}_{1x}, v_{1y}\mathbf{u}_{1y}, v_{1z}\mathbf{u}_{1z}\}$, the specification of $\mathbf{v}$ in system U_2 can be found by multiplying $\mathbf{v}_1$ by a transformation matrix, A_{12}:

$$\mathbf{v}_2 = A_{12}\,\mathbf{v}_1. \qquad (16)$$

Insert 2. Matrix multiplication

Multiplication of a vector by a matrix: $\mathbf{v}^* = A\,\mathbf{v}$

If the matrix A is a 3 x 3 matrix with terms

$$\begin{matrix} A_{11} & A_{12} & A_{13} \\ A_{21} & A_{22} & A_{23} \\ A_{31} & A_{32} & A_{33} \end{matrix}$$

The components of the result vector are

$$v^*_x = A_{11}\,v_x + A_{12}\,v_y + A_{13}\,v_z$$
$$v^*_y = A_{21}\,v_x + A_{22}\,v_y + A_{23}\,v_z$$
$$v^*_z = A_{31}\,v_x + A_{32}\,v_y + A_{33}\,v_z$$

Multiplication of a matrix B by a matrix A, written as C = AB, must be defined so that $\mathbf{v}^* = C\mathbf{v} = (AB)\mathbf{v} = A(B\mathbf{v})$. To satisfy this requirement, Matrix B is interpreted as a set of column vectors $\{\mathbf{v}_1, \mathbf{v}_2, \mathbf{v}_3\}$ and Matrix C is interpreted as a set of column vectors $\{\mathbf{v}^*_1, \mathbf{v}^*_2, \mathbf{v}^*_3\}$, where $\mathbf{v}^*_1 = A\mathbf{v}_1$, etc. Note that this multiplication operation is not commutative: AB is not equal to BA.

A transformation matrix can be used to provide information about translation of the origin of the coordinate systems, but for changes in specification of a vector that possibility is not used, and the transformation matrix is a rotation matrix. To find the components of the transformation matrix, consider the case where $\mathbf{v}_1$ is the unit vector $\mathbf{u}_{1x}$, represented by $\{1, 0, 0\}$. Then we see that $\{A_{11}, A_{21}, A_{31}\}$ represents the components of the unit vector $\mathbf{u}_{1x}$, in the U_2 coordinate system. These quantities are also referred to as the direction cosines of the $\mathbf{u}_{1x}$ vector in the U_2 coordinate system, and they can be represented as dot products $\{\mathbf{u}_{2x} \bullet \mathbf{u}_{1x}, \mathbf{u}_{2y} \bullet \mathbf{u}_{1x}, \mathbf{u}_{2z} \bullet \mathbf{u}_{1x}\}$. The remainder of the matrix can be established in the same manner.

The same procedure can be used to obtain A^{-1}, the inverse of A, such as the matrix A_{21} that converts a vector expressed as coordinates in system U_2 to coordinates in system U_1. We then discover that the inverse of a rotation matrix, such as A, is simply its transpose A^T -- the matrix

formed by converting rows into columns [Hines and Blum, 1983]. This greatly simplifies computation of the inverse of A. Another important property of a rotation matrix is that the sum of the squared components of each row or column equals 1.0 (the normalization condition).

Any transformation by a rotation matrix is equivalent to rotation of the coordinate system by an angle θ around some axis represented by a unit vector **a** [see Goldstein, 1980]. The rotation formula, for rotation of a vector in a fixed coordinate system [Goldstein, 1980], can be written in matrix form, with the components of **a** represented by $\{a_x, a_y, a_z\}$:

$$A_{12} = \begin{matrix} a_x a_x(1-\cos\theta) + \cos\theta, & a_x a_y(1-\cos\theta) + a_z\sin\theta, & a_x a_z(1-\cos\theta) - a_y\sin\theta \\ a_x a_y(1-\cos\theta) - a_z\sin\theta, & a_y a_y(1-\cos\theta) + \cos\theta, & a_y a_z(1-\cos\theta) + a_x\sin\theta \\ a_x a_z(1-\cos\theta) + a_y\sin\theta, & a_y a_z(1-\cos\theta) - a_x\sin\theta, & a_z a_z(1-\cos\theta) + \cos\theta \end{matrix} \qquad (17)$$

This matrix can be found in many computer graphics texts. It was derived in Brokaw [2002] from the rotation formula in Goldstein [1980], and a more complete derivation is given in Rogers and Adams [1976]. If the coordinate system U_2 is rotated to obtain U_1, A_{21} is formed by using the rotation formula with $\theta \rightarrow -\theta$ (Goldstein, 1980) and $\{a_x, a_y, a_z\}$ expressed in the U_2 system. Then A_{12} is the transpose of A_{21}, which is equivalent to using $+\theta$, as written in equation (16).

For very small θ, A_{12} becomes the infinitesimal transformation matrix:

$$\begin{matrix} 1, & a_z\theta, & -a_y\theta \\ -a_z\theta, & 1, & a_x\theta \\ a_y\theta, & -a_x\theta, & 1 \end{matrix} = I + ds \begin{matrix} 0, & \theta_z, & -\theta_y \\ -\theta_z, & 0, & \theta_x \\ \theta_y, & -\theta_x, & 0 \end{matrix} = I + ds \begin{matrix} 0, & \theta, & -\theta \\ -\theta, & 0, & 0 \\ \theta, & 0, & 0 \end{matrix} \qquad (18)$$

I represents the identity matrix, with $A_{ij} = 0$ except for $A_{11} = A_{22} = A_{33} = 1$, and the θ or θ, θ terms in the matrices are recognizable as the matrix form of equations (6). Note that the infinitesimal transformation matrix is only an approximation, which does not satisfy the normalization condition. Also, the infinitesimal matrix is antisymmetric, while the finite transformation matrix (equation 17) does not have this property.

Given the coefficients of a finite rotation matrix, the recommended method (Glassner, 1990) for extracting the rotation parameters is to calculate

$$\cos\theta = (A_{11} + A_{22} + A_{33} - 1)/2, \qquad (19)$$

and then use the arccos function to extract θ. Although the arccos function does not reveal whether θ is + or -, this is unimportant in the present context because the curvature is considered to always be +. The arccos function can introduce significant ambiguities if the magnitude of θ is greater than

□, and these must be dealt with. The **a** vector components can then be obtained from

$$a_x = (A_{23} - A_{32})/2\sin\theta, \text{ etc.} \qquad (20)$$

1.5 Drawing a circular helix

The simplest computer graphics representation of any curve is as a set of line segments drawn between points that lie on the curve. By placing the points sufficiently close together, the curve will appear smooth, within the resolution of the graphics display device. Although it is important to have methods that will work with any bent shape of an axoneme, the circular helix will be used as an illustration.

1.5.1 Construction method 1

To draw the curve, this method uses equations (14) to find the X Y Z coordinates for points that are spaced at equal intervals, Δs, along the arc length of the curve. The curve is then approximated by drawing a straight line segment between each pair of adjacent points. The points between segments can be referred to as joints, where the segmental representation of the curve bends. The length Δs_s of each straight segment is **P**(j+1) − **P**(j) , which can be calculated from equation (14):

$$(\Delta s_s)^2 = r^2(2(1 - \cos(2\pi\Delta s/S)) + (h\Delta s/rS)^2)$$
$$= \rho^2(2(1 - \cos(2\pi\Delta s/S)) + (2\pi\Delta s/\tau S)^2)/(\rho^2 + \tau^2)^2 \qquad (21).$$

For sufficiently small Δs, the length of each segment becomes close to Δs. For example, using ρ = τ = 0.2 rad μm^{-1} gives a helix with a radius of 2.5 μm and an arc length S of 22.21 μm , Drawing this with S divided into 20 segments, with Δs = 1.1105 μm gives Δs_s = 1.1082 μm , which is only 0.2% less than Δs. This curve is shown in Figure 2.

Although method 1 can be used when the curve is specified by constant values of curvature and torsion, using equations (11 to 13) to convert equation (14) to functions of ρ and τ, it can only be used if the values of ρ and τ are constant, so that it is known in advance that the result will be a circular helix. Other methods must be used if ρ and τ are variable functions of s.

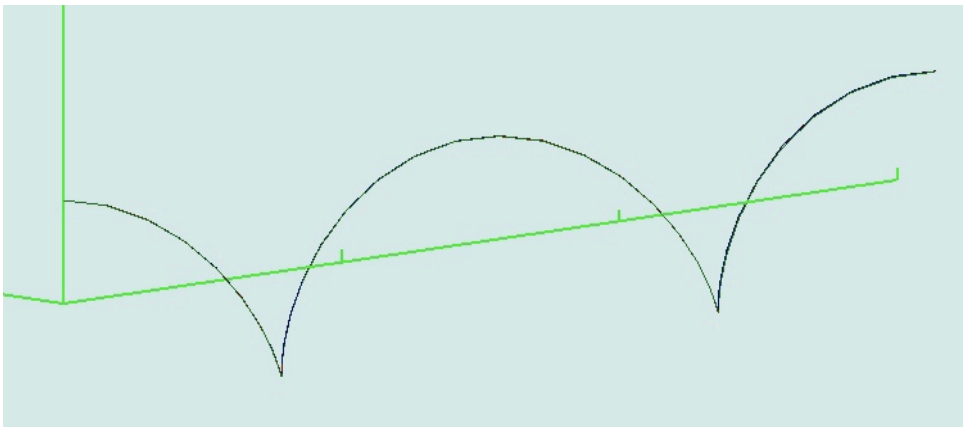

Figure 2. Helices drawn in three dimensions using the three construction methods outlined in section 1.5. This helix is generated by $\Omega = \Omega = 0.2$ rad/μm. This gives an arc length of 22.21 μm in one turn of the helix. For plotting, 40 segments, each with a length of 1.1105 μm, were used, to give two turns of the helix. For methods 2 and 3 to give results that match the result from Method 1, the initial position of the helix must be at {0, r, 0}, where r is the calculated radius of the helix, the orientation of the first segment must be in the direction {–1, 0,1}, and the rotation at the first joint is half the rotation angle at subsequent joints. The z axis, shown in green, runs along the axis of the helix, with markers at 10 μm intervals.

1.5.2 Construction method 2

Alternatively, when given Ω and Ω as functions of s, the curve can be drawn by a more general method that does not presuppose that the result is a helix. At joint j at the end of segment j, the Frenet-Serret coordinate frame rotates through an angle DΔs around the axis given by the Darboux vector, which has magnitude D. If A is a transformation matrix that can be used to transform from the Frenet-Serret coordinate frame to the global X Y Z coordinate frame, then A[j+1] = RA[j], where R is the rotation matrix corresponding to the rotation DΔs specified by the Darbaux vector. In forming the rotation matrix, the Darbaux vector must first be transformed into the global coordinate system by using matrix A[j]. A[j+1] can then be used to transform the segment vector {0, 0, Δs} from the Frenet-Serret **t n b** coordinate frame into the global coordinate system, so that this segment can be added to the position of joint j to get the position of joint j+1.

If Δs is sufficiently small so that the difference between Ωs_s and Ωs can be neglected, this is an accurate method when Ω and Ω are constant. If desired, it can be made more exact by using a value of Ωs_s calculated as in equation (20). Figure 2 shows the helix constructed by this method.

When Ω and Ω vary, and are given specified values at each joint, this is only an approximate method. The orientation of the tangent vector at the joints where the Darbaux vector is calculated does not correspond exactly to the orientation of either of the segments. However, for the purposes of this paper, and other work with axoneme models such as Brokaw (2002), it is assumed that Ωs is

small enough that this method provides a good enough approximation, so that it is not necessary to derive a more refined method.

1.5.3 Construction method 3

Method 3 is used when the space curve is specified by a vector function of arc length, $\Omega(s)$. The transformation matrix A is now used for transformation between the body x y z coordinate system and the global X Y Z coordinate system. If the magnitude and direction of Ω in the body coordinate system is specified as a function of s, then Ω, as the vector sum $\Omega_x + \Omega_y + \Omega_z$ is used instead of the Darbaux vector for rotating the transformation matrix. If necessary, a specification of the torsion component $d\tau/ds$ as a function of s can be integrated to obtain Ω_x and Ω_y, given a starting orientation for Ω. This method, in effect, accomplishes rotation by the Darbaux vector in two steps, as the sum of two rotations. The Darbaux vector is resolved into its Ω and Ωcomponents. The Ω component is used to rotate the curvature vector in the local coordinate system, and the Ω component is then used to rotate the transformation matrix, which is then used to transform {0, 0, Ωs} from the body coordinate system to the global coordinate system, as in method 2.

As shown in Figure 2, these three methods give indistinguishable results, if the initial position and orientation of the first segment are properly specified. Methods 2 and 3 can also be computed using the infinitesimal rotation matrices of equation (18), but much smaller Ωs steps, at least 1/100 of the steps used for Figure 2, must be used.

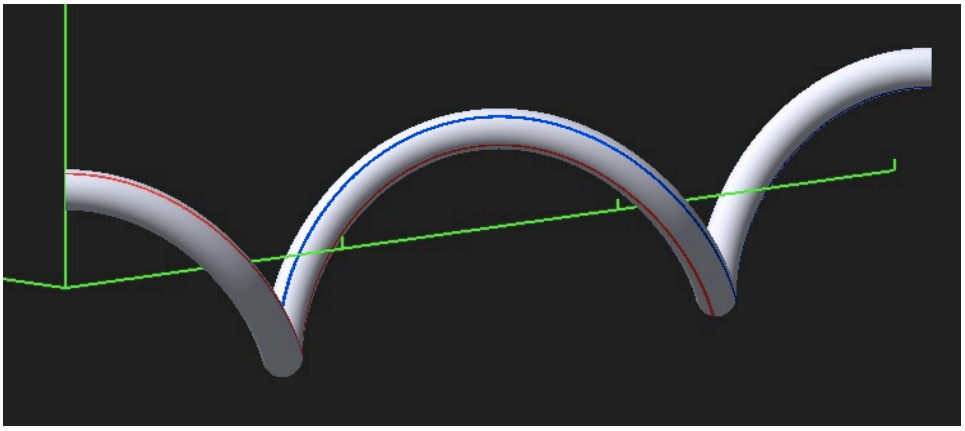

Figure 3. A cylinder constructed by Construction method 3. Its axis is the helical space curve drawn in Figure 2. Two elements in the surface of the cylinder have been colored to show how they rotate around the cylinder as the cylinder bends. This rotation is the writhe of the curve.

1.6 Writhe

Figure 3 shows a cylinder that is bent into a helix and drawn using construction method 3, for a case where $\Omega_z = 0$. Figure 3 shows two full turns of the helix, and two of the elements in the surface of the cylinder. In one full turn of a helix, the curvature vector and the entire Frenet-Serret frame must rotate around the helix axis through 2π radians and return to its original orientation:

$$DS = 2\pi. \tag{22}$$

However, the rotation of the curvature vector in the local xyz coordinate system is ΩS. The additional rotation of the curvature vector results from rotation of the xyz coordinate system, which is illustrated in Figure 3 by the path of elements in the surface of the cylinder. This rotation is the writhe of the curve, and for one turn of a regular circular helix the writhe must equal

$$W = 2\pi Wr = 2\pi \, \Omega S = (D - \Omega) S. \tag{23}$$

When indicated by the symbol Wr, writhe is usually measured by the terminal rotation at the end of a curve in units corresponding to 2π rotations. Here, the symbol W is used to represent writhe measured in radians. For the helix drawn in Figures 2 and 3, D = 0.2828 rad/μm, so $D - \Omega$ = 0.0828 rad/μm, and for each turn of the helix, equation (23) gives a value of W = 1.84 rad. For this helix, the writhe can also be calculated by using equations (19) and (20) to extract the rotation vector from the rotation matrix at the end of one full turn, where the next segment should be parallel to the basal segment. The z component of this rotation vector gives a value of W = 1.83 rad.

Writhe is a rotation that results from the bending of the cylinder. It may be most familiar in the context of a plumber's snake, used for pipe cleaning. This is a cylindrical structure designed to have a high twist resistance and a low bending resistance. The high twist resistance allows it to transmit torque, or rotation, applied to one end, without absorbing the torque as twist. The low bending resistance allows it to bend easily to match bends in a pipe. When its bending is determined by the bends in the pipe, it can transfer rotation from one end to the other. However, in the absence of an enclosing pipe, application of a torque to rotate one end of the structure when rotation of the other end is restrained usually causes it to bend, or "writhe" into a complex, more or less helical, conformation, because the bending resistance is low. The bending produces writhe, causing the end of the structure to rotate and neutralize any twist put into the structure by the applied torque. In general, knowing the amount of rotation put into one end of the structure is not sufficient to determine the conformation that results from bending. Writhe is also important for analysis of the structure of DNA and other flexible polymers [see Maggs, 2001].

1.6.1 Writhing rate

Writhe is usually measured by the terminal rotation, in units corresponding to full 2π rotations, and no attempt is made to define writhe at points along the curve. For the regular circular helix, it might be expected that writhe increases linearly in a regular manner, and the writhing rate would be dW/ds = D □ □ However, this expectation is just a speculation, without a formal basis. Evidence to support this idea can be obtained by examination of the structure drawn in Figure 3. With appropriate rotations and translations it can be seen that the slope of an element as it wraps around the bent cylinder is the same at all positions along the length (Figure 4). However, this indication that the writhe increases linearly along the length is not supported by calculation of the writhe.

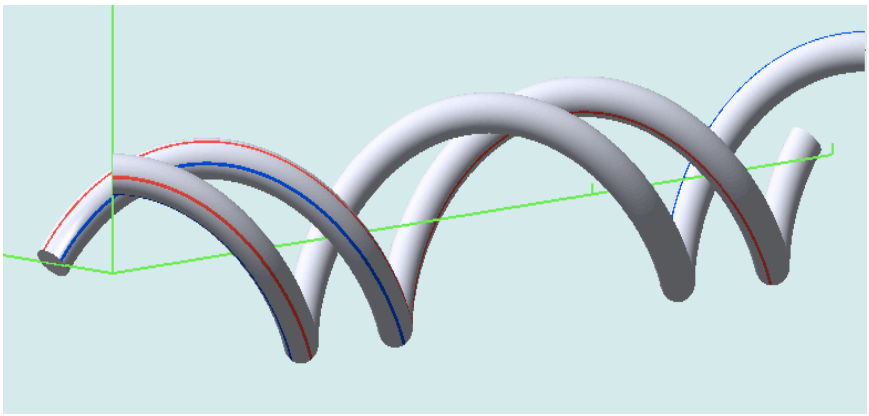

Figure 4. The helix in Figure 3 has been redrawn, before and after a 90 degree rotation around the Z axis. This allows comparison of the rotation of the red element in the first 1/4 of a helix turn with the blue element in the second 1/4 of a helix turn.

It might be expected that the writhe at points along a curve obtained by construction method 3 should be obtainable from the transformation matrices A[j] that were used to construct the curve. These matrices transform the local xyz coordinate system to the basal XYZ coordinate system. At segment j, the cross product of the segment j vector and the basal segment vector provides the rotation required to make the segment vector parallel to the basal segment. Since this rotation vector is in the plane perpendicular to the segment vectors, it has no Z component. This rotation is used to rotate the transformation matrix A[j]. The transformation matrix then contains only the rotation around the Z axis, and extracting the rotation vector from it using equations (19) and (20) yields {0, 0, W}. If there is twist, the rotation obtained from the transformation matrix is the sum of the twist and the writhe. Complications arise in using the arcsin function to obtain the rotation from the cross product if the rotation is greater than π/2 radians, but these can be dealt with. The writhing rate can

then be approximated as

$$dW/ds = (W[j] - W[j-1])/\Delta s. \quad (24)$$

This calculation does not reveal a constant writhing rate, but instead a writhe that increases sigmoidally with length (s/S). Although the writhe of a half turn of a helix is half of the writhe of a full helix turn, the writhe of the first 1/4 of a helix is much less than 1/4 the writhe of a full helix. The writhing rate obtained from the transformation matrix by this method is not a local property of the curve, but depends upon the starting position from which the writhe is calculated. This result is consistent with the interpretation of a helix as a circular trajectory on the unit tangent sphere [Maggs, 2001]. One turn of the helix corresponds to a full circle on the tangent sphere, with a radius equal to $\sin(\theta_H)$. The writhe is equal to the enclosed surface area, which is a spherical zone with area $2\pi(1-\cos(\theta_H))$. For less than one complete turn of the helix, the area is enclosed by an arc and a geodesic line that returns to the origin. Computations of this area (see below) give results identical to the results obtained from the transformation matrix, as described in the preceding paragraph. The arc represents the sum of the multiple rotations at each segment, and the geodesic line represents the single rotation that returns the orientation of a segment to its starting orientation. This representation makes it easy to see that the writhing rate, which is the rate of increase of the enclosed area corresponding to a partial helix, is maximal when s = S/2.

1.6.2 Computation of writhe of a partial helix from surface area on the unit tangent sphere

The writhe is equal to the difference between the area of a fraction s/S of the spherical zone and the area of an isosceles spherical triangle with apical angle $2\pi s/S$ and a base formed by the geodesic line connecting the two ends of the arc.

$$W = 2\pi s(1-\cos(\theta_H)/S - (2\theta_\beta + 2\pi s/S - \pi), \quad (25)$$

where θ_β is the interior angle of intersection of the geodesic line forming the base of the triangle with the geodesic line from the pole of the sphere to the origin of the arc. This angle θ_β is obtained from the cross product of the normals to the planes containing these geodesic lines. These normals will be defined in an x,y,z coordinate system with the y axis corresponding to the polar axis of the sphere, and the x,y plane bisecting the apical angle. The plane containing the base of the triangle contains the z axis and makes an angle θ_α with the polar axis of the sphere. This angle θ_α is given by

$$\alpha = \arctan(\sin(\beta_H)\cos(\tau s/S)/\cos(\beta_H)). \quad (26)$$

The normal to this plane is then $\{\cos(\alpha), \sin(\alpha), 0\}$. The plane containing the geodesic line from the pole to the origin of the arc contains the y axis and has a normal $\{-\sin(\tau s/S), 0, \cos(\tau s/S)\}$. The magnitude of the cross product of these two unit normal vectors is then equal to the sine of the angle α needed in equation 25. This method works directly for s<=0.5S. For larger s, the calculated value using s = S–s can be subtracted from the writhe for the full helix. Figure 5 shows results of this computation for one turn of the helix in Figure 3.

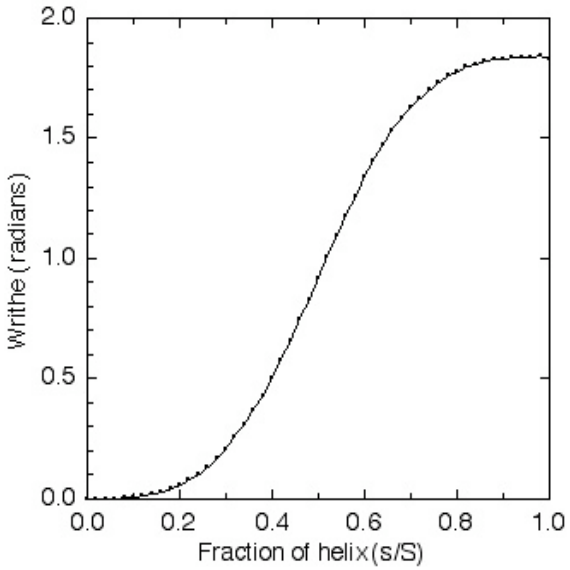

Figure 5. Calculation of writhe within one turn of the helix drawn in Figure 3, using the surface area method of section 1.6.2

1.6.3 Writhe of a non-helical space curve

The computation described in section 1.6.2 depends on the trajectory on the sphere being a circle, and is therefore specific to a circular helix. Computation of the writhe from the transformation matrices is possible for more general space curves, because it makes no assumptions about the shape of the curve. It is therefore important that the transformation matrix method is validated, at least for the circular helix, by the surface area method in section 1.6.2. If there is twist, it must be subtracted from the rotation returned from the transformation matrix, in order to obtain the writhe. The utility of the writhe calculated in this manner remains to be established.

1.7 The inverse problem

Given a series of points **P**[j] for j = 0 to N, with a constant spacing Δs between **P**[j] and **P**[j−1], how do we obtain the parameters that describe the bending of the curve? The more general version of this problem has been examined in detail by Crenshaw et al.[2000] with particular attention to the use of noisy data points. Here, equations are given for only the simplest problem, without noise and with constant Δs. If a segment vector **T**[j] = **P**[j]−**P**[j−1], the magnitude of the curvature at joint j can be estimated by vector subtraction, as in equation (2):

$$\kappa[j] = |(\mathbf{T}[j+1] - \mathbf{T}[j])|/\Delta s^3 = \arcsin((\mathbf{T}[j+1] \times \mathbf{T}[j])/\Delta s^2)/\Delta s \qquad (27)$$

The cube of Δs appears in equation (27) instead of Δs because the **T** vectors are not unit vectors. The direction of the rotation of the segment vectors at joint [j] is the direction of $\boldsymbol{\kappa}[j] = T[j] \times T[j+1]$. The unit vector in this direction is $\boldsymbol{\kappa}[j]/|\boldsymbol{\kappa}[j]| = \mathbf{b}$, the unit binormal vector of the Frenet-Serret frame. **b**[j] and **b**[j+1] are both perpendicular to **T**[j+1], and therefore are coplanar, so the torsion can be estimated in a similar manner as

$$\tau[j+1] = \sin|\mathbf{b}[j+1] - \mathbf{b}[j]| \, \mathbf{T}[j+1]/\Delta s. \qquad (28)$$

These steps give the tangent vector and torsion for a segment, while the curvature is calculated for a joint. To put all of the quantities in the same context, the curvature value for a segment can be obtained by averaging curvature values for the start and end of the segment. In this manner, the parameters of the curve in the local Frenet-Serret frame can be obtained from 4 adjacent **P**[j] points. To obtain a description of the curve in terms of κ[j] in a body xyz frame, the torsion must be integrated from the basal end where the initial orientation of the curvature vector relative to the body xyz frame is known.

Part 2. Dynamics

The analysis of ciliary and flagellar movement requires not only analysis of the shape of the axoneme, but also analysis of how this shape changes through time. The common assumption is that the time evolution of the shape can be obtained by solving a partial differential equation (PDE) that represents the balance between active forces generated within the axoneme and passsive forces that resist bending. When the only resisting forces are simple internal resistances of the axonemal structure, the equation can be fully established within the body coordinate systems, as functions of the curvature of the axoneme [Brokaw, 2002]. Solving the PDE to obtain the curvature vector κ(s,t)

as a function of both s and time provides the information needed to draw the shape of the axoneme at successive time points.

This calculation is insufficient, because cilia and flagella operate in a fluid environment, and the viscous resistances provided by this environment are usually an important part of the force balance equation. The viscous resistances arise from the motion of the axoneme relative to the fluid, and their calculation depends upon the velocities of the axoneme, expressed in a global coordinate system. To incorporate both these global velocities and the local functions of curvature into the force balance equation requires a method for relating the velocities to rates of change of curvature, or vice versa.

As in part 1, the discussion will be developed around the example of a circular helix.

2.1 Helical bending waves

2.1.1 Waves

If f(s) is a periodic function of length, s, then f(s−vt) represents a wave that travels in the positive direction along s as a function of time. The propagation velocity along s is represented by the scalar velocity parameter, v.

2.1.2 Wave motion by rotation of a circular helix

Using equation (14), we can write

$$X = -r \sin(2\pi(s-vt)/S), \quad Y = r \cos(2\pi(s-vt)/S), \quad Z = hs/S. \qquad (29)$$

The Z term is not changed, since this is not a periodic function of s. The temporal period T = S/v. Figure 6 shows the results of computing the helix shown in Figure 2 at t=0 and tv/S = 0.25, or t = 0.25T. The helical curve rotates around the Z axis with an angular velocity = $-2\pi/T$, and every point on the curve is moving in a plane perpendicular to the Z axis, with a velocity with a magnitude of $2\pi r/T$. This type of rotation of a rigid helix is used for propulsion by bacteria, but it is not a bending wave.

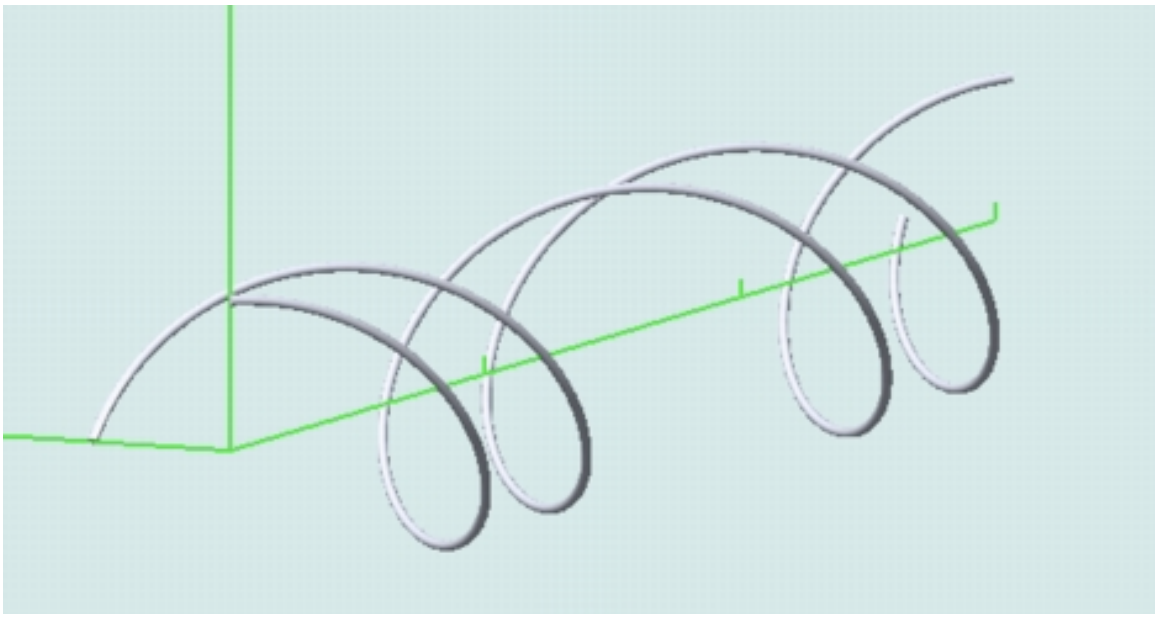

Figure 6. Rotation of a circular helix according to equation 29. The helix parameters are the same as in Figures 2. 3 and 4.

2.1.3 Helical bending waves

A helical bending wave results by specifying the components of the curvature vector function as {□cos(□(s–vt)), □□sin(□(s–vt)), 0}. Figure 7 shows the results of computing the shape of the curve for time intervals such that □v□t = □/4. The curves were calculated using the procedure in section 1.5.3, with curvature vectors adjusted for each time point. The velocity of a point P(s) can be calculated as the limit of (P(s,t+□t) –P(s,t))/ □t, as □t goes to 0. As an alternative, for small values of □t the shape at t + □t can be calculated by using values of □ obtained from □ = □ (t) + (d□/dt) □t. For the circular helix, starting at t = 0, □={□cos(□s), □□sin(□s), 0} and d □ /dt = {□□v sin(□s), □□v cos(□s), 0}. Then, at t = □t, the shape can be calculated using □={□cos(□s) +□□v sin(□s) □t, □□sin(□s) + □□v cos(□s) □t , 0}. Figure 8 shows that these two methods give the same result, at least for the value of □t used for this figure. When using larger □t, the results obtained by addition of □ and d□/dt components could be improved by normalizing the length of the □ vector after adding the d□/dt components (not shown).

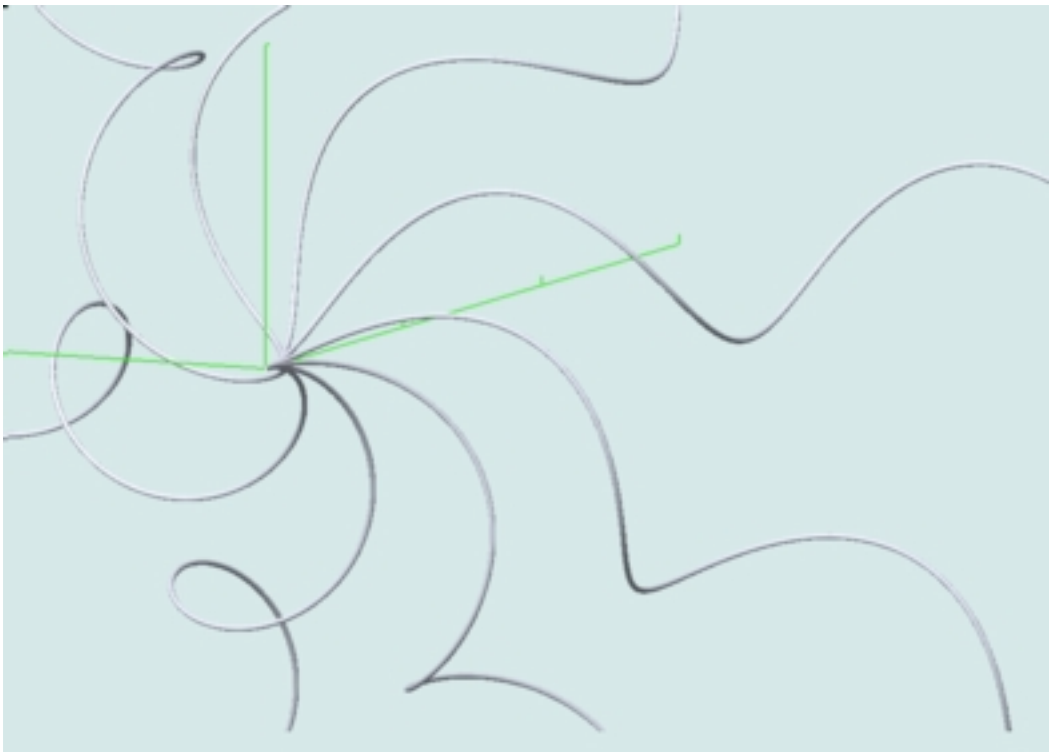

Figure 7. Propagation of a helical bending wave, with the first segment fixed at the origin, along the +X axis of the global XYZ coordinate system. The shape is recalculated at time intervals such that the curvature vectors rotate by $\pi/4$ radians between each time point.

A similar result is obtained by rotation of the rigid helix calculated at $t = 0$ in $\pi/4$ radian steps around the Z axis of its first segment. The velocity of a point P(s) can then be calculated as W **X** P(s,t), where W is the angular velocity of the first segment. Alternatively, a similar result is obtained by bending at the first joint that causes an equivalent rotation of all of the segments beyond the first joint. These results are surprising, because we expect that the propagation of bending from t to $t+\Delta t$ will require bending at each joint, not just rotation or bending at the first joint. Understanding these results provides the key to developing the more general method that is needed to obtain the velocity of a point P from knowledge of κ and $d\kappa/dt$ at t.

2.1.4 Addition of bends is not simple.

A better understanding can be obtained by examing a simplified model, with only a minimal number of segments, using bends of $\pi/2$ radians. The model is a cylinder, with one element of the cylinder marked along the length, corresponding to the local +y axis. Starting with the cylinder on the Z axis of the global coordinate system, with the local +y axis corresponding to the local +Y axis, the marked element runs along the top, or +Y, surface of the cylinder. Shape 1 will be

calculated at t = 0. At t = 0 and joint 1, the curvature vector is in the +x and +X directions. This corresponds to $\theta = 0$, with $\kappa_x = \kappa \cos(0) = \kappa$ and $\kappa_y = \kappa \sin(0) = 0$. The bend at the first joint then $= \kappa\, ds = \pi/2$. This bend causes segment 2 to point downwards, in the –Y direction, with the marked element facing the +Z direction.

Shape 2 at $t = \Delta t$ is calculated by starting over again with the cylinder on the Z axis. Δt is chosen so that $\theta = +\pi/2$ radians, $\kappa_x = \kappa \cos(\pi/2) = 0$ and $\kappa_y = \kappa \sin(\pi/2) = \kappa$. The curvature vector has rotated by the angle θ and is now in the +y and +Y direction. The bend at joint 1 now causes segment 2 to point to the left, in the +X direction, with the marked element remaining on top, in the +Y direction.

To go from t = 0 to $t = \Delta t$, we can attempt to transform Shape 1 into Shape 2 by rotating segment 1 by $\pi/2$ radians, using a rotation vector in the +z and +Z direction, which causes segment 2 to swing up from the –Y direction to the +X direction, as desired. Alternatively, we can bend Shape 1 by $\pi/2$ radians in the +Z direction at joint 1, which also causes segment 2 to swing up to the +X direction. However, in both of these cases, the marked element remains facing the +Z direction, and does not end up facing the +Y direction, as in the original calculation of Shape 2. To complete the transformation to match Shape 2, an additional rotation of segment 2 at joint 1, by $\pi/2$ radians in the –X direction, is required. The second rotation does not change the position of segment 2, or contribute to the velocity at joint 2. In other words, to match the single rotation in the +Y direction (for $t = \Delta t$), a sequence of 3 rotations, not 2, is required, if the sequence is initiated with a rotation in the +X direction (the t = 0 bend).

The second rotation required at joint 1 for transformation of Shape 1 to Shape 2 is in the local –z direction of segment 2. If we advance now to joint 2, we would expect to transform from Shape 1 to Shape 2 by bending by $\pi/2$ radians in the +z direction at joint 2. This bending would exactly cancel the second rotation at joint 1. For a regular helix, this cancellation continues through the remainder of the length, and the result is that only the first rotation of the first segment, or bend at the first joint, remains. As far as the shape of the space curve is concerned, this single rotation of segment 1 is then sufficient to complete the transformation from Shape 1 to Shape 2. However, the paired +z and –z rotations must be performed in order to end up with the marked element correctly oriented throughout the length so that it displays correctly the writhe of the curve throughout its length. This method works for a circular helix, where the required rotations are equal to the rotations of the curvature vector, given by $d\theta/dt$. It would require major modification for the planar case, where there are changes in the magnitude of κ, but no rotation of the curvature vector. Fortunately, a better method is available.

2.1.5 A better method

Now that it is recognized that two rotations are required at each joint, a second method for transformation from Shape 1 to Shape 2 is apparent. Using the same simple example introduced in 2.1.4, the first rotation at joint 1 is a rotation in the +y = +Y direction. This rotation does not change the position of segment 2, but merely rotates segment 2 around its z axis so that the marked element faces in the +X direction. The second rotation is a +Z rotation at the first joint. This +Z rotation brings segment 2 up to the +X direction, with the marked element on top, in the +Y direction, corresponding to the correct result for t = Δt. This +Z rotation corresponds to a +y rotation, transformed to the global coordinate system by using A[2], the transformation matrix calculated for segment 2 of Shape 1. The same pair of +y,+y rotations is used at each succeeding joint, with the first rotation transformed by A[j] and the second rotation transformed by A[j+1]. This second method is more convenient than the method described in 2.1.4, because the required rotation is obtained directly from the components of d□/dt It is easy then to see that this method will work for the two-dimensional case only if this sum of rotations is divided by 2.0. A formal proof of this method remains to be developed, but Figure 8 demonstrates that this method, including the division by 2.0, gives correct results.

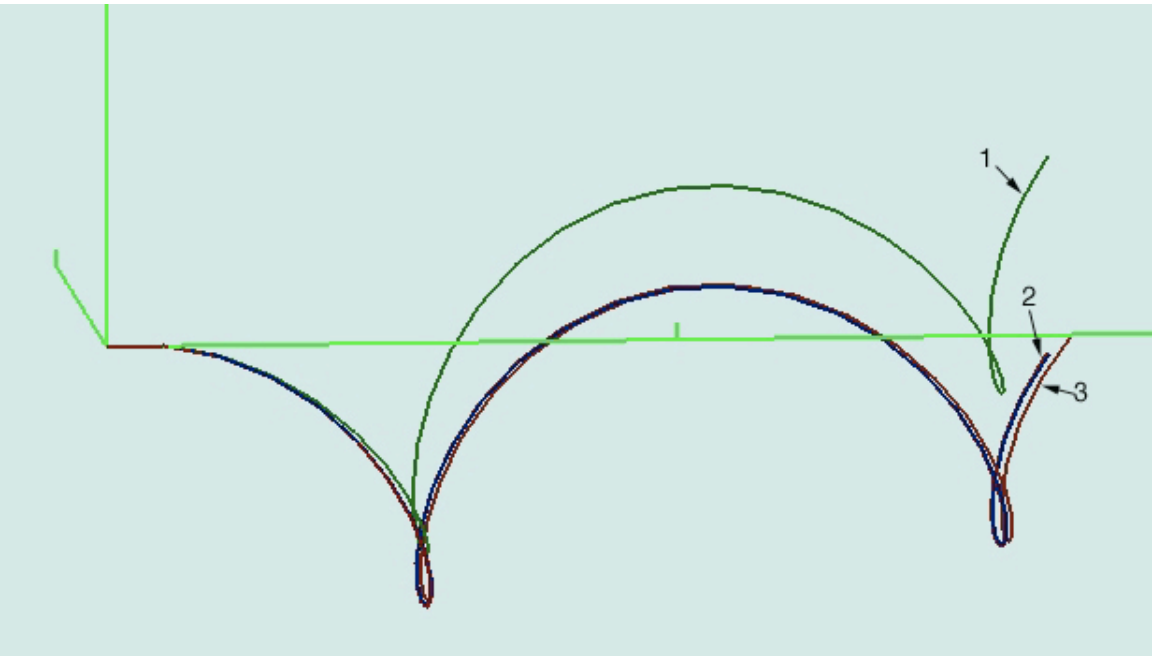

Figure 8. Calculation of a helical curve, with the first segment fixed at the origin and aligned with the +X axis, at two time points. As in previous examples, the helix is calculated with □ = □= 0.2 rad/μm. The green curve (1) corresponds to t = 0. The other curves are calculated for t = □t = 8 seconds, with v = 0.10 μm/sec. The blue curve (2) is actually the superposition of three curves,

calculated with the methods in sections 2.1.3 and 2.1.5. The red curve (3) is the result obtained when the calculation of section 2.1.5 is performed using a single rotation, instead of the two rotations described in section 2.1.5. Note that the error is especially evident as a velocity in the +Z direction, which should not be produced by rotation of segment 1 around its z axis.

2.2 Application to generalized bending in flagellar simulations

In the computer simulations of flagellar movement by Brokaw [2002], velocities for calculation of viscous resistances were calculated using only one rotation at each joint. These velocities were obviously incorrect, and resulted in incorrect results for the swimming velocity of a flagellum. To change the flagellar simulations to incorporate the method in 2.1.5, the only change is that the transformed $d\phi/dt$ components, $\phi'[k]^*$ needed for equation (14) of Brokaw [2002] are obtained by transforming $\phi'[k]$ by 0.5(A[k]+A[k+1]) instead of by A[k]. In a typical simulation, the velocities calculated by this method differ by only about 1% from velocities calculated from the difference between the shapes calculated before and after a time step. Errors introduced by this difference in velocities would be small compared to errors in the hydrodynamic approximations, such as the resistance coefficient method of Gray and Hancock [1955]. At least 95% of the incorrect swimming velocity calculated for cases where the swimming velocity should be 0 is eliminated by this improvement. For computations with the very small values of Δt that are required with stochastic modeling of dynein kinetics, the error in the computed swimming velocity is reduced to less than 0.1 μm per beat cycle. Figure 8 also shows the magnitude of the error introduced by the single rotation method originally used in Brokaw [2002]. For the example in Figure 8, the change between t and $t+\Delta t$ is much larger than would be used during flagellar simulations.

References

Brokaw, C. J. (1990) The sea urchin spermatozoon. Bioessays 12: 449-452.

Brokaw, C. J. (2002) Computer simulation of flagellar movement. VIII. Coordination of dynein by local curvature control can generate helical bending waves. Cell Motil. Cytoskel. 53:103-124.

Crenshaw, H. C., Ciampaglio, C. N., and McHenry, M. (2000) analysis of the three-dimensional trajectories of organisms: Estimates of velocity, curvature, and torsion from positional information. J. exptl. Biol. 203: 961-982.

Glassner, A. S. (1990) Graphics Gems. San Diego, Academic Press

Goetz, A. (1970) Introduction to Differential Geometry. Reading, MA, Addison Wesley Pulbishing Company.

Goldstein (1980) Classical Mechanics. 2nd ed. Reading, MA, Addison Wesley Pulbishing Company.

Gray, J. (1955) The movement of sea-urchin spermatozoa. J. exptl. Biol. 32: 775-801.

Gray, J., and Hancock, G. J. (1955). The propulsion of sea-urchin spermatozoa. J. exptl. Biol. 32: 802-814.

Gueron, S., and Levit-Gurevich, K. (2001). A three-dimensional model for ciliary motion based on the internal 9+2 structure. Proc. Roy. Soc. Lond. B 268: 599-607.

Gueron, S. and Liron, N. (1993) Simulations of three-dimensional ciliary beats and cilia interactions. Biophys. J. 65: 499-507.

Hines, M., and Blum, J. J. (1983) Three-dimensional mechanics of eukaryotic flagella. Biophys. J. 41: 67-79.

Hines, M., and Blum, J. J. (1984) On the contribution of moment-bearing links to bending and twisting in a three-dimensional sliding filament model. Biophys. J. 46: 559-565.

Maggs, A. C. (2001) Writhing geometry at finite temperature: Random walks and geometric phases for stiff polymers. J. Chem. Phys. 114: 5888-5896.

Phillips, D. M. (1969). Exceptions to prevailing pattern of tubules (9+9+2) in the sperm flagella of certain insect species. J. Cell Biol. 40: 28-43.

Phillips, D. M. (1971). Insect flagellar tubule patterns. Theme and variations. In B. Baccetti, ed., Comparative Spermatology, pp 264-273. New York, Academic Press.

Rogers, D. F., and Adams, J. A. (1976) Mathematical Elements for Computer Graphics. New York, McGraw-Hill.